Journal of Environmental Management 232 (2019) 236–242

Contents lists available at ScienceDirect

Journal of Environmental Management

journal homepage: www.elsevier.com/locate/jenvman

Research article

# Bacteriological synthesis of iron hydroxysulfate using an isolated *Acidithiobacillus ferrooxidans* strain and its application in ametryn degradation by Fenton's oxidation process

S. Bhaskar[a], Basavaraju Manu[a], M.Y. Sreenivasa[b,*]

[a] Department of Civil Engineering, National Institute of Technology Karnataka, Surathkal, P.O. Srinivasanagar, Mangalore, 575025 D.K, India
[b] Department of Studies in Microbiology, University of Mysore, Mysuru, Karnataka, India

ARTICLE INFO

*Keywords:*
*Acidithiobacillus ferrooxidans*
Fenton's process
Jarosite
Herbicide
Ametryn

ABSTRACT

The investigation reports the application of biogenic jarosite, an iron hydroxy sulfate mineral in Fenton's Oxidation process. Ametryn, a herbicide detrimental to aquatic life and also to human is treated by Fenton's oxidation process using synthesized iron mineral, jarosite. The jarosite synthesis was carried out by using an isolated *Acidithiobacillus ferrooxidans* bacterial strain with ferrous as an iron supplement. The isolated strain was characterized by molecular techniques and biooxidation activity to ferrous to ferric iron was checked. On Fenton's treatment ametryn degradation upto 84.9% and COD removal to the extent of 56.1% was observed within 2 h of treatment and the reaction follows the pseudo first order kinetics with the curve best fit. The slight increase in kinetic rate constant on jarosite loading rate increase from 0.1 g/L to 0.5 g/L with $H_2O_2$ dosage of 100 mg/L confirms that jarosite has a catalytic role in the removal of ametryn. Mass spectroscopy analysis of treated synthetic ametryn solution at various intervals reveal the degradation follows dealkylation and hydroxylation pathway with the formation of three major intermediate compounds discussed here.

## 1. Introduction

Environmental technology has made a significant contribution to science by finding the ways to degrade most of the recalcitrant hazardous wastes. Most of the pesticides and herbicides like endrin, dieldrin, aldrin and triazine compounds used in the agriculture pose hazard to environment as they become micro organic contaminants on reaching surface and groundwater bodies by surface runoff and infiltration (Wang et al., 1996). Many combinations of treatment techniques including chemical and biological treatment have been tried to get rid of the hazardous waste. Ametryn is one of the widely used herbicide in the agriculture to control broad leaf and grassy weeds to which most of the crops like sugarcane, popcorn, paddy etc are more prone. The extent of herbicides like ametryn usage, as a derivative of s – triazine compound in agriculture is increasing during the present decade (Lopez et al., 1997). Sangami and Manu (2017) has discussed about the composition and structure of ametryn. The greater affinity of ametryn sorption towards ground water and surface water may pose hazard to aquatic and human health (Kolpin et al., 1998; Kasozi et al., 2012). Transmittance of this herbicide from soil to water bodies leads to toxic condition to most of the aquatic species including algae (Gaggi et al., 1995). Fenton's oxidation treatment which has proven to be most effective and economic in treating triazine compounds (Arnold et al., 1995; Gaggi et al., 1995). During this process iron plays a major role as a catalyst thereby enhancing reaction kinetics. Jarosite is an iron hydroxy sulfate precipitate found naturally in the soil bearing iron sulfide under acidic condition which can be used as a replacement for the chemical iron which is chemically synthesized from ferric sulfate under acidic condition (Dutrizac and Kaiman, 1976; Pappu et al., 2006). However, chemical synthesis of iron is not advisable as it is not eco-friendly. Utilization of biologically synthesized jarosite as catalyst in Fenton's oxidation process has been studied by a limited number of researchers (Yan et al., 2017). The biological synthesis of jarosite using acidophilic bacterium such as *Acidithiobacillus ferrooxidans* in laboratory has got importance in this respect (Daoud and Karamanev, 2006; Gramp et al., 2009; Yan et al., 2017).

*Acidithiobacillus ferrooxidans* is an acidophilic chemolithotropic proteobacteria commonly found in acid mines bearing iron sulfide. It plays an important role in oxidizing ferrous iron and synthesizing such minerals as jarosite and schwertmannite which could be used as

* Corresponding author.
*E-mail addresses:* baskarmalwanitk@gmail.com (S. Bhaskar), bmanu@nitk.ac.in (B. Manu), sreenivasamy@gmail.com, mys@microbiology.uni-mysore.ac.in (M.Y. Sreenivasa).

https://doi.org/10.1016/j.jenvman.2018.11.048
Received 26 July 2018; Received in revised form 12 November 2018; Accepted 13 November 2018
Available online 23 November 2018
0301-4797/ 

catalyst in Fenton's like processes to treat hazardous organic compounds. It is of interest of microbiologist and biochemist to know with paleochemistry to investigate the oxidation pathways of this bacteria. However the application of biogenic jarosite as a substitution for chemical iron in the Fenton's treatment for the degradation of ametryn has not been studied yet. The present study encompasses the isolation and characterization of *Acidithiobacillus ferrooxidans* from natural acid mine drainage followed by the biosynthesis of jarosite using an isolated strain and degradation of ametryn using synthesized jarosite as a catalyst in Fentons reaction.

## 2. Material and methods

### 2.1. Isolation and characterization of Acidithiobacillus ferrooxidans

Acid mine drainage (AMD) samples were collected from coal mines, located in North eastern part of India. Onsite pH and temperature was measured during sampling. Samples were carefully taken to the laboratory for isolation. Isolation media used is modified 9K media (Wood and Kelly, 1993). All the components of the medium were autoclaved except ferrous sulfate which was filter sterilized before mixing to avoid precipitation on heating. The medium was adjusted to pH 3 prior to sterilization. Under sterilized condition the media was inoculated with 4% AMD samples, incubated for 15 days in incubator shaker at 30 °C and at 180 rpm. Samples from enrichment medium were spread on solid media prepared with the same media composition with 2% agarose additional supplement for solidification. The plates were incubated at 30 °C for five days. Screening of the developed colonies was done by streaking to fresh plates till pure single colony was obtained.

### 2.2. Isolation of genomic DNA

*Acidithiobacillus ferrooxidans* cells of 10–12 days old culture were harvested by centrifuging 50 ml broth at 8000 rpm for 10 min. Cell pellets were washed twice with PBS (NaCl 137 mmol/L, KCl 7 mmol/L, $Na_2HPO_4$ 10 mmol/L, $KH_2PO_4$ 1.8 mmol/L) and incubated for 60 min at 37 °C. The solution was added with 400 µL of lysis buffer and 15 µL of proteinase K and incubated for 60 min at 55 °C. The solution was centrifuged for 15 min at 4 °C with the supplement of 400 µL phenol:-chloroform (1:1). The upper aqueous layer was taken out and 400 µL of chloroform:isoamyl alcohol (24:1) was added following the centrifugation at 10,000 rpm for 15 min and incubation at −20 °C for 60 min. After incubation 5 µL of 5 M NaCl and twice the volume of absolute alcohol were added to the collected supernatant. The mixture was centrifuged at 14,000 rpm after 3 h to precipitate DNA. Precipitated DNA was rinsed with 70% alcohol, air dried and pellets were suspended in nuclease free water and stored at −20 °C for further analysis (Chennappa et al., 2014).

### 2.3. 16s rDNA sequencing

PCR amplification was carried out with universal primers, specific primers and rusticynin enzyme specific primers (Chen et al., 2009a,b; Escobar et al., 2008; Hall et al., 1996; Ilieva et al., 2011).

PCR amplification with the universal primers was carried out to 50 µL volume with the following composition: 4 µL of DNA extract, 5 µL of PCR buffer, 5 µL of $MgCl_2$, 4 µL of dNTP's, 2 µL of 24F primer and 2 µL of 1492R primer, 0.25 µL of Taq polymerase and 27.75 µL of nuclease free water. The gene amplification process was programmed for initial denaturation with 94 °C for 5 min each cycle followed by 30 cycles, each cycle was conditioned 94 °C for 30 s, 55 °C for 45 s, 72 °C for 90 s and final extension with 72 °C for 7 min. While the PCR amplification with species specific and rusticynin enzyme specific primers was carried out with the mixture of 0.5 µL dNTP's, 2.5 µL of Taq buffer, 1.5 µL of $MgCl_2$, 0.5 µL of Taq polymerase, 2 µL of DNA extract, 0.25 µL of F1 thio (sense) primer and 0.25 µL of R1 thio (antisense) primer, rus_F and rus_R (in case of rusticynin specific) to the final volume of 25 µL adding 17.7 µL of nuclease free water. The process was programmed for initial denaturation step with 94 °C for 5 min followed by 30 cycles, each cycle conditioned at 94 °C for 30 s, 57 °C for 45 s, 72 °C for 90 s and 72 °C for last 7 min. The PCR product obtained was run on ethidium bromide stained agarose gel prepared with 1.5% agarose immersed in 1X TAE buffer. The band formation was confirmed with gel doc instrument. The primers used in the study and corresponding annealing temperature are shown in Supplementary Table 1.

The sequencing was done for the amplicon of 16s rDNA using F1_Thio (sense) and R1_Thio (antisense) primers approximately 900bp and analyzed. Phylogenetic analysis was carried out by constructing phylogenetic tree with MEGA 5.1 software by neighbor joining algorithm. The nucleotide sequence was submitted to NCBI Genebank.

### 2.4. Bacteriological synthesis of jarosite

Jarosite, an iron hydroxyl sulfate mineral was bacteriologically synthesized in modified 9K medium with 0.144 M ferrous iron supplement to get total volume of 1000 ml. Culture medium was adjusted to pH 3.0 by adding 1N $H_2SO_4$ prior to incubation. *Acidithiobacillus ferrooxidans* cells of 100 ml volume with the cell density of $1.0 \times 10^7$ cells/ml were inoculated to the media and incubated in shaker at 180 rpm with 30 °C for 12 days. The precipitate formed on iron oxidation was filtered using Whatman's filter paper No.4, washed with acidified water of pH 2 and dried in oven to get jarosite powder which was stored for further use. The precipitate formed was characterized by X-ray diffraction.

### 2.5. Biogenic jarosite catalyzed Fenton's oxidation of ametryn

Iron catalyzed Fenton's oxidation of ametryn was carried out with 5 mg/L of initial herbicide concentration to mimic the field ametryn concentration (Sangami and Manu, 2016, 2017). Ametryn solution prepared in the laboratory was taken in a conical flask to which of jarosite powder was added in an incremental rate. The solution was adjusted to pH 3 using 1N $H_2SO_4$ and allowed 10 min for proper mixing to ensure uniform distribution of jarosite powder in the solution prior to $H_2O_2$ addition. Investigation was conducted with experimental conditions of jarosite (0.1 g–1 g) and $H_2O_2$ dosage (100 mg/L – 1000 mg/L). Samples were drawn at regular intervals for analysis. During sampling, each time 1 ml of sodium thiosulphate was added to halt the reaction (Khan et al., 2009). All the experimental analysis was conducted in triplicates. The ANNOVA is performed to the obtained experimental results using origin pro software.

### 2.6. Scanning electron microscopic (SEM) analysis

Morphological feature of isolated *Acidithiobacillus ferrooxidans* strain was studied with scanning electron microscopy. Bacterial cells were fixed at 5 °C for 90 min with 5% gluteraldehyde in acidic buffer pH 2.5 stained with 0.25% uranyl acetate at 4 °C for 1 h and air dried before examination. The morphology of biosynthesized jarosite was studied with the oven dried powdered precipitate. The sample was mounted on aluminium stub using double sided carbon tape, sputter-coated with gold and visualized using a S-3400N scanning electron microscope (Hitachi, Japan).

### 2.7. Analytical procedure

Ametryn concentration was measured by a high-performance liquid chromatograph (HPLC) employing an Agilent 1200 with a C18 reverse phase column (pore size 3.5 µm, 100 × 0.46 cm), using water and methanol (in the ratio of 58:42) as mobile phase injected with a flow rate of 1.0 ml/min employing diode array detector (DAD). The volume

of sample used for the measurement was 20 μm with retention time of about 10min (Sangami and Manu, 2017). Chemical oxygen demand (COD) measurement was by colorimetric method as per 5220D of Standard Methods for Examination of Water and Wastewater (Apha, 1995). The $H_2O_2$ consumption was measured using UV–Vis spectrophotometer (Eisenberg, 1943). Concentration of ferric iron was measured by potassium thiocyanate method using UV-Spectrophotometer (Woods and Mellon, 1941). For intermediate identification, samples after submitting to the degradation processes were analyzed by electrospray ionization/mass spectrometry using a positive electrospray ionization mode (ESI–MS), and a LC/MSDTOF (Agilent Technologies) mass spectrometer operated with the following parameters: capillary 4500 V; nebulizer 3.0 bar; drying gas 12.0 L/min; gas temperature 180 °C. Spectra were acquired over m/z 20–1000 range. The pH was monitored by digital pH meter.

## 3. Results and discussion

### 3.1. Isolation and purification of bacterial strain

A dark reddish colony showing gram negative, rod-shaped, oxidase and catalase positive bacterial colonies was isolated after plating acid mine drainage sample on modified 9K media (Table 1). The isolate showed efficient growth at pH 3 and at 30 °C temperature on modified 9K medium with ferrous being the energy source (Wang et al., 2014; Yang et al., 2014; Chen et al., 2017; Wood and Kelly, 1993). Further, scanning electron microscopic studies revealed that, the rod shaped filamentous bacterial cell structure with round ends, with 423 nm–47.3 nm diameter occurring as single or aggregated (Fig. 1 a). Polymerase chain reaction (PCR) amplified DNA on agarose gel run showed then band size as 900 bp. Dendogram representation of 16S rDNA based on BLAST algorithm was prepared and compared with previous published data (Hallberg and Lindström, 1994). The isolated bacterial strain is closely related to *Acidothiobacillus ferrooxidans*, a chemolithotrophic gamma proteobacteria and the sequence of the isolate has been assigned the accession number MG271840 by NCBI Genebank.

Phylogenetic analysis revealed that the isolated colonies are the members of acidophilic bacteria which are having autotrophic mode of metabolism. Isolates matched up to 99% to the identified members. The optimal tree with the sum of branch length = 0.07797533 is shown Fig. 2. The tree is drawn to scale, with branch lengths in the same units as those of the evolutionary distances used to infer the phylogenetic tree. The evolutionary distances were computed using the Maximum Composite Likelihood method and are in units of number of base substitutions per site. The analysis involved 18 nucleotide sequences. All positions containing gaps and missing data were eliminated. Evolutionary analyses were conducted in MEGA7 (Tan et al., 2007; Wu et al., 2014). The characteristic features and nearest phylogenetic match is shown in Table 1.

### 3.2. Biosynthetic jarosite formation and its characterization

On biooxidation of ferrous sulfate by *Acidithiobacillus ferrooxidans* BMSNITK17 cell suspensions at pH 3, yellow iron precipitates were formed with the solution containing 0.144 M ferrous sulfate and 0.06 M potassium. Meraune and Vargas (2003) observed that below pH 5 bacterial oxidation of ferrous is predominant over chemical oxidation. The rate of proton diffusion hinders below pH 2.5 as the ferric oxide layer formed allows the accumulation of precipitates on the bacteria thus reducing the rate of oxidation. Huang and Zhou (2012) observed that the rate of oxidation of ferrous iron on mineral phase of jarosite precipitate depends on local pH changes. In the present study jarosite precipitation was observed after inoculation of bacteria into ferrous sulfate medium within 10 days of incubation at low pH. During the biooxidation of ferrous sulfate not much variation in the pH was

**Table 1**
Colony characteristics and nearest phylogenetic match.

| Isolate | Colony Morphology | [a]Nearest Match | Identity (%) | Isolation medium | Inferred Metabolism | Phylogenetic affiliation | Gene bank accession number |
|---|---|---|---|---|---|---|---|
| *Acidithiobacillus ferrooxidans* BMSNITK17 | Rusty orange brownish appearance | *Acidithiobacillus ferrooxidans* ATCC23270 | 94 | Ferrous sulfate | Iron oxidation/chemolithotrophic | Gama proteobacteria | MG271840 |
| | | *Acidithiobacillus ferrooxidans* ATCC33020 | 93 | | | | |

[a] Nearest relative to the isolate obtained was determined by BLAST method.

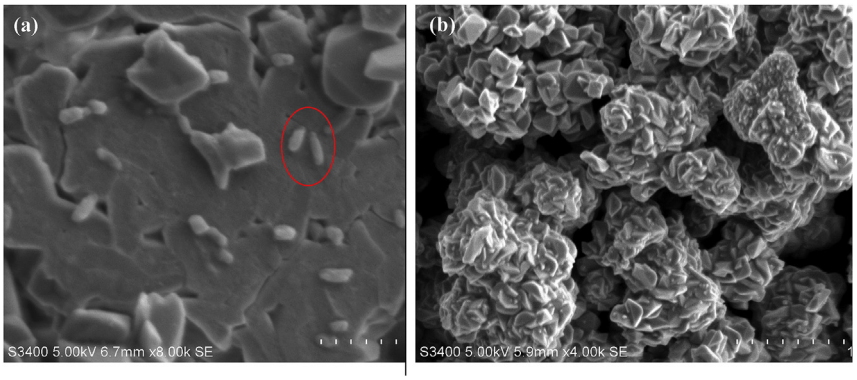


**Fig. 1.** SEM images showing a) *Acidithiobacillus ferrooxidans* b) Biogenic jarosite.

observed. However, the reason for this could be attributed that the changes in pH during the biooxidation of ferrous iron was hindered by the hydrolysis of ferric. At 0.144 M iron concentration and 0.06 M potassium concentration in the medium yellow precipitate is formed. The formed jarosite precipitates are ternary solids with monovalent cation $K^+$ (Jones et al., 2014; Bigham et al., 2010).

$$3Fe^{3+} + K^+ + 2SO_4^{2-} + 6H_2O \rightarrow KFe_3(SO_4)_2(OH)_6 + 6H^+$$

During the initial four days, the biooxidation rate is slightly high and this may be due to the formation of ferric iron prior to jarosite precipitate under low pH condition. On biooxidation of ferrous sulfate by the *Acidithiobacillus ferrooxidans*, the formation of jarosite precipitation is less in quantity. Iron precipitate attaches to the extracellular polymeric substances (EPS) during the biooxidation and also formation of EPS-$Fe^{3+}$ complex lowers the precipitates formation quantitively (Huang and Zhou, 2012). Less jarosite precipitate formation can be attributed to the drop in pH to less than 2 in seven days (Daoud and Karamanev, 2006). Iron precipitate is seen as agglomerated particles resembling rose petals with smooth interface through SEM images observed (Fig. 1b). The XRD analysis of particles exhibits six characteristic broad peaks 24.44, 29.14, 35.15, 39.47, 47.74 and 50.04 at an angle 2Θ with unit cell parameter *c* being 17.034 A°. Signal

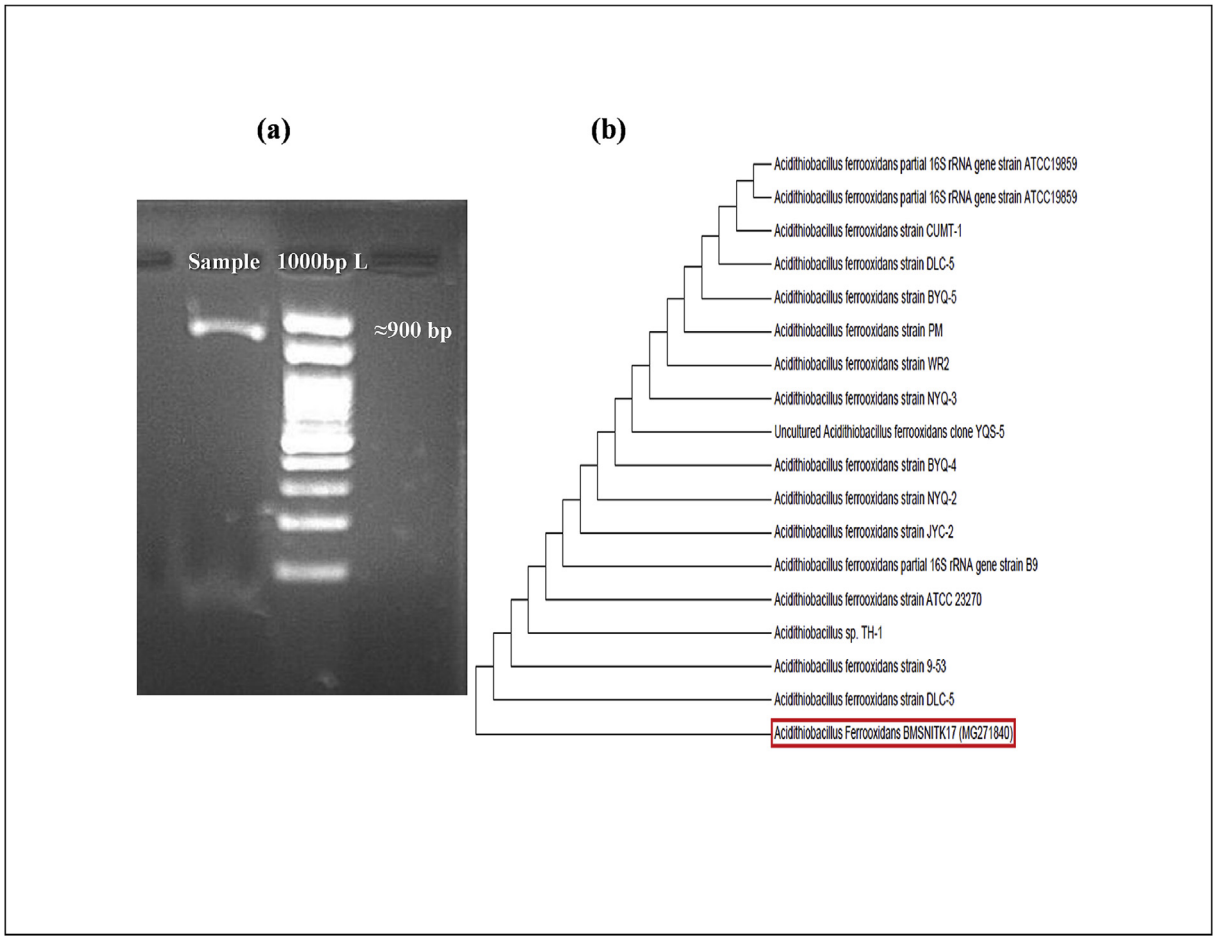


**Fig. 2.** a) Agarose gel showing an amplicon of 16s rDNA of the isolate, L – 1000bp ladder, Sample – *Acidithiobacillus ferrooxidans* BMSNITK17 b) Dendogram representation of phylogeny of *Acidithiobacillus ferrooxidans* obtained. Strain belong to this study is shown highlighted in the box. Parenthesis number is obtained Genebank number.

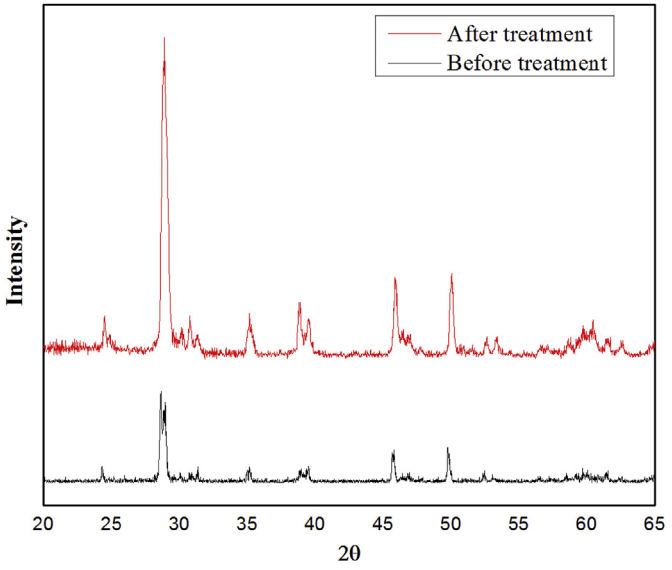


**Fig. 3.** XRD pattern of Biogenic jarosite before and after treatment.

to background ratio of XRD patterns in Fig. 3 showing lowest ratio indicating its poor crystallinity (Chen et al., 2016, 2017). The formed precipitates are said to be jarosite (PDF No 01-071-1777). As per the previous studies the formation of jarosite was observed by providing ferrous iron as supplement along with potassium (Yan et al., 2017). The formation of jarosite has been confirmed in the present study by observing broad peaks at 2Θ. Supplementary Fig. 1 dissipates the EDS data, which is matching with the XRD results for the identification of jarosite phase (Chowdhury et al., 2017). Specific surface area of the synthesized biogenic jarosite is 1.62 $m^2/g$ as per BET analysis. Elemental composition and specific surface area reveals that the jarosite is formed directly on biooxidation of ferrous sulfate medium provided (Wang et al., 2006). The characteristics of biogenic synthesized jarosite are tabulated in Table 2.

### 3.3. Catalytic degradation of ametryn by biogenic jarosite

Degradation of ametryn by jarosite catalyzed heterogeneous Fenton like process was investigated. Initially no removal of ametryn was observed without the addition of $H_2O_2$ in solution containing ametryn and jarosite. The degradation however starts slowly on the addition of $H_2O_2$ initiating the reaction. High removal efficiency upto 84.90% is found with jarosite dosage of 0.5 g/L and $H_2O_2$ dosage of 100 mg/L at pH 3.0 and temperature 30 °C. The COD removal was 51.6% in first 120 min. This signifies the better oxidation rate. The increase of $H_2O_2$ from 100 mg/L to 200 mg/L, 500 mg/L and 1000 mg/L did not show significant change with 0.5 g/L of jarosite load. However further increase in $H_2O_2$ dosage more than 100 mg/L might not lead to shortening of induction period as per the previous studies (Yan et al., 2017). During the reaction, there was slight increase in pH 3.0 to 4.21. Fenton's reaction is active in acidic pH as the condition favors the oxidation and production of OH radicals. If the pH turns basic the hydrated ferrous ions gets transformed into colloidal ferric species i.e ferric hydroxyl complexes which results in drop of degradation efficiency (Kang and Hwang, 2000; Burbano et al., 2005; Khan et al., 2009). The lower pH observed during the treatment favored the catalytic degradation of ametryn producing high quantity OH radicals. Previous studies have shown that even though when pH is greater than point of zero charge biosynthesized jarosite consumes hydroxyl radicals resulting in pH drop, the hydroxyl bridges of jarosite re-polymerize to further drop in pH (Yan et al., 2017). The increase in the rate of ametryn degradation on increase in jarosite load from 0.1 g/L to 0.5 g/L indicates the high iron concentration favors the Fenton's oxidation as it helps in $H_2O_2$ decomposition to produce more OH radicals by the acceleration of active sites on the catalyst. In the present study, 84.90% of ametryn degradation is observed. The kinetic rate increased nearly by 1.2 times by the increase in catalyst loading from 0.1 g/L to 0.5 g/L. However, increase in jarosite loading more than this dosage did not show any significant changes. Fig. 4 graphically represents the effect of $H_2O_2$ on the oxidation process and Fig. 5 represents the variation in ferric and total iron contents during the process. Kinetic studies show that pseudo-first order rate kinetic model fits the process (Chen et al., 2017). Fig. 6 shows the kinetic fit. The ANNOVA performed for the data obtained reveals the error of 0.227% at 0.5 g/L jarosite loading and 100 mg/L of $H_2O_2$ dosage which is considered as the optimized condition in this study. Overview of Fenton's degradation of ametryn is tabulated in Table 3.

### 3.4. Intermediates formed on degradation of ametryn

Supplementary Table 2 shows the intermediates formed during the Fenton's oxidation of ametryn using biogenic jarosite. Ametryn on this degradation process follows alkylic oxidation and hydroxylation pathways. With two dealkylation intermediates 2 – acetamido – 4 (iso propylamino) – 6 – (methylthio) – s triazine (SDIT) and 2 – amino – 4 (ethylamino) – 6 – (methylthio) – s triazine (SEAT) resulting from the oxidation of alkyl group in the lateral chain to form acetamide-aldehyde compounds and one hydroxylation intermediate 2 – ethylamino – 4 hydroxy - 6 (isopropylamino) – s triazine (OIET) identified. The OH radicals produced attacks the lateral chain of heterocycle in the dechlorination hydroxylation process to form OIET. Chen et al., 2017 claims deisopropylation of ametryn gives SEAT with m/z value 186.08 identified in the present study. The m/z value of 198.13 in the present study confirms the formation of dechlorinated hydroxylated intermediate 2 – ethylamino – 4 hydroxy - 6 (isopropylamino) – s triazine (OIET) from the initial hydroxylation of ametryn which later follows dealkylation pathway. Dechlorinated product undergo dealkylation process to form dechloro - dealkylated biproducts 2 – hydroxyl-4-isopropylamino-6-diamino triazine (OIAT) and 2-hydroxly-4,6-diamino triazine (OAAT) with m/z value 170.10 and 128.05 respectively; OAAT being the final product of fenton's oxidation. The intermediate compounds formed in this study within 20 min of treatment. Strong electron donating effect of methylthio group reliable for hydroxyl radical attack makes the ametryn more susceptible for Fenton's oxidation compare to the other herbicides (de Oliveira et al., 2018).

## 4. Conclusions

*Acidithiobacillus ferrooxidans,* an iron oxidizing bacterium was isolated from acid mine drainage sample obtained from North eastern coal field, India. The same isolate was used to synthesis jarosite. This biogenic jarosite found to have a catalytic role in the Fenton's oxidation of ametryn by mineralization and releasing OH radicles to attack the

**Table 2**
Characteristics and elemental composition of Biogenic jarosite synthesized in the study.

| Mineral | Color, Shape | Identical chemical formula | Molecular weight | Fe (Wt %) | S (Wt %) | O (Wt %) | K (Wt %) |
|---|---|---|---|---|---|---|---|
| Jarosite | Yellow, Rose petal shapes | $KFe_3(SO_4)_2(OH)_6$ | 500.81 | 11.54 | 20.46 | 66.82% | 1.18 |

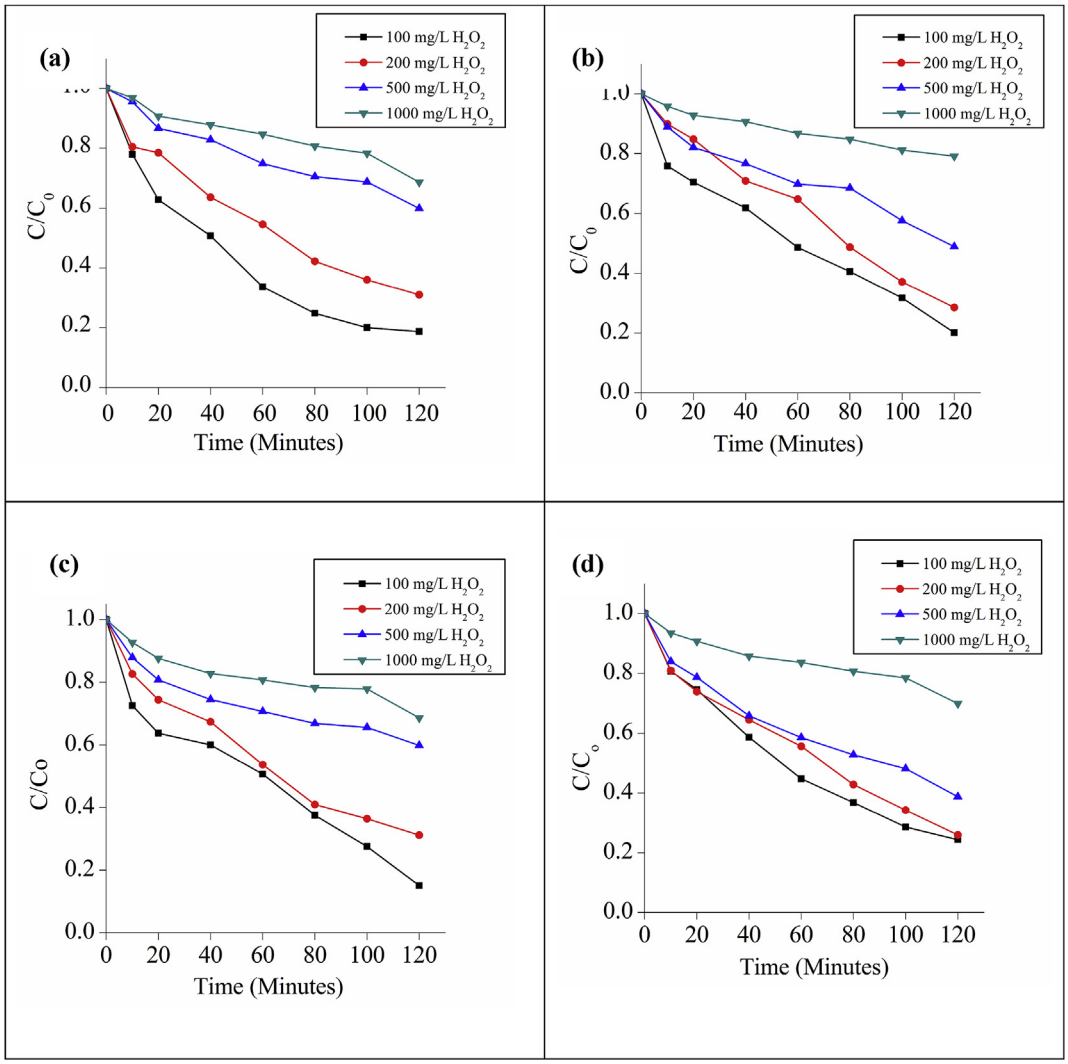


**Fig. 4.** Effect of $H_2O_2$ concentration on the process at different jarosite loading a) 0.1 g/L jarosite b) 0.2 g/L jarosite c) 0.5 g/L jarosite and d) 1.0 g/L jarosite.

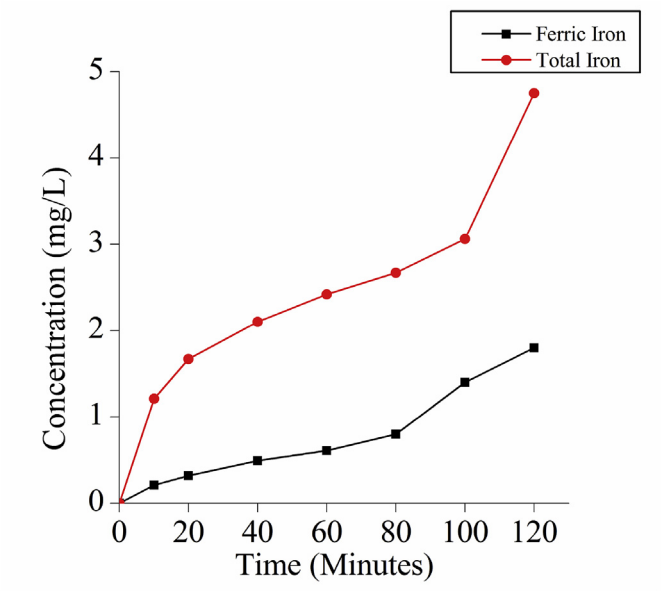


**Fig. 5.** Variation of Ferric iron and total iron during the process.

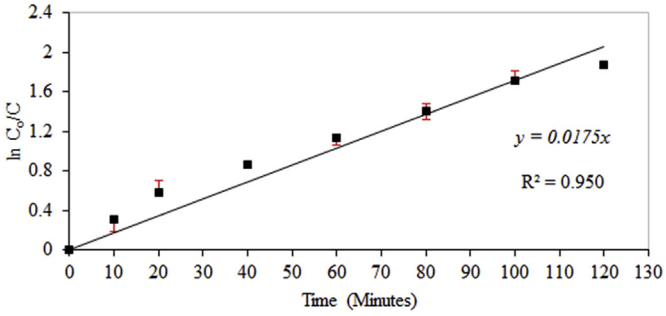


**Fig. 6.** First order kinetic model fit ln $C_o/C$ versus time.

lateral bonds in the ametryn. Efficiency of jarosite in degradation of ametryn is found to be 84.9%. MS analysis shows the intermediates formed during the process reveals the degradation pathway follows methylthio oxidation and hydroxylation steps. Higher efficiency in target pollutant removal within short period of time retrofits the use of biogenic jarosite in Fentons oxidation process over commercially available iron.

## Acknowledgment

The first author would like to thank MHRD, Govt. of India, India for

**Table 3**
Fenton's oxidation of ametryn.

| Catalyst | First order kinetic regression $R^2$ | First order rate constant k ($min^{-1}$) | Ametryn degradation efficiency (%) | COD Removal rate (%) |
|---|---|---|---|---|
| Jarosite | y = 0.0175 × (0.9506) | 0.0175 | 84.90 | 51.6 |

providing research fellowship. We thank IOE, University of Mysore for providing the instrumentation facility to conduct experiments.

## Appendix A. Supplementary data

Supplementary data to this article can be found online at https://doi.org/10.1016/j.jenvman.2018.11.048.

## References


Apha, A., 1995. WPCF, Standard Methods for the Examination of Water and Wastewater. American Public Health Association, Washington, DC.

Arnold, S.M., Hickey, W.J., Harris, R.F., 1995. Degradation of atrazine by Fenton's reagent: condition optimization and product quantification. Environ. Sci. Technol. 29 (8), 2083–2089.

Bigham, J.M., Jones, F.S., Özkaya, B., Sahinkaya, E., Puhakka, J.A., Tuovinen, O.H., 2010. Characterization of jarosites produced by chemical synthesis over a temperature gradient from 2 to 40 C. Int. J. Miner. Process. 94 (3–4), 121–128.

Burbano, A.A., Dionysiou, D.D., Suidan, M.T., Richardson, T.L., 2005. Oxidation kinetics and effect of pH on the degradation of MTBE with Fenton reagent. Water Res. 39 (1), 107–118.

Chennappa, G., Adkar-Purushothama, C.R., Suraj, U., Tamilvendan, K., Sreenivasa, M.Y., 2014. Pesticide tolerant Azotobacter isolates from paddy growing areas of northern Karnataka, India. World J. Microbiol. Biotechnol. 30 (1), 1–7.

Chen, H., Yang, B., Chen, X., 2009a. Identification and characterization of four strains of *acidithiobacillus ferrooxidans* isolated from different sites in China. Microbiol. Res. 164 (6), 613–623.

Chen, C., Yang, S., Guo, Y., Sun, C., Gu, C., Xu, B., 2009b. Photolytic destruction of endocrine disruptor atrazine in aqueous solution under UV irradiation: products and pathways. J. Hazard. Mater. 172 (2–3), 675–684.

Chen, T., Liu, Z., Yao, J., Hao, H., Chen, F., 2016. Fenton-like degradation comparison of s-triazine herbicides in aqueous medium. Clean. - Soil, Air, Water 44 (10), 1315–1322.

Chen, F., Xie, S., Huang, X., Qiu, X., 2017. Ionothermal synthesis of Fe3O4 magnetic nanoparticles as efficient heterogeneous Fenton-like catalysts for degradation of organic pollutants with H2O2. J. Hazard. Mater. 322, 152–162.

Chowdhury, M., Shoko, S., Cummings, F., Fester, V., Ojumu, T.V., 2017. Charge transfer between biogenic jarosite derived Fe3+ and TiO2 enhances visible light photocatalytic activity of TiO2. J. Environ. Sci. 54, 256–267.

de Oliveira, D.M., Cavalcante, R.P., da Silva, L.D.M., Sans, C., Esplugas, S., de Oliveira, S.C., Junior, A.M., 2018. Identification of intermediates, acute toxicity removal, and kinetics investigation to the Ametryn treatment by direct photolysis (UV 254), UV 254/H 2 O 2, Fenton, and photo-Fenton processes. Environ. Sci. Pollut. Control Ser. 1–19.

Daoud, J., Karamanev, D., 2006. Formation of jarosite during Fe2+ oxidation by *Acidithiobacillus ferrooxidans*. Miner. Eng. 19 (9), 960–967.

Dutrizac, J.E., Kaiman, S., 1976. Synthesis and properties of jarosite-type compounds. Can. Mineral. 14 (2), 151–158.

Eisenberg, G., 1943. Colorimetric determination of hydrogen peroxide. Ind. Eng. Chem. Anal. Ed. 15 (5), 327–328.

Escobar, B., Bustos, K., Morales, G., Salazar, O., 2008. Rapid and specific detection of *Acidithiobacillus ferrooxidans* and Leptospirillum ferrooxidans by PCR. Hydrometallurgy 92 (3–4), 102–106.

Gaggi, C., Duccini, M., Bacci, E., Sbrilli, G., Bucci, M., El Naby, A.H., 1995. Toxicity and hazard ranking of s-triazine herbicides using microtox® two green algal species and a marine crustacean. Environ. Toxicol. Chem. 14 (6), 1065–1069.

Gramp, J.P., Wang, H., Bigham, J.M., Jones, F.S., Tuovinen, O.H., 2009. Biogenic synthesis and reduction of Fe (III)-hydroxysulfates. Geomicrobiol. J. 26 (4), 275–280.

Hall, J.F., Hasnain, S.S., Ingledew, W.J., 1996. The structural gene for rusticyanin from Thiobacillus ferrooxidans: cloning and sequencing of the rusticyanin gene. FEMS Microbiol. Lett. 137 (1), 85–89.

Hallberg, K.B., Lindström, E.B., 1994. Characterization of Thiobacillus caldus sp. nov., a moderately thermophilic acidophile. Microbiology 140 (12), 3451–3456.

Huang, S., Zhou, L., 2012. Fe2+ oxidation rate drastically affect the formation and phase of secondary iron hydroxysulfate mineral occurred in acid mine drainage. Mater. Sci. Eng. C 32 (4), 916–921.

Ilieva, R., Groudeva, V., Iliev, M., 2011. PCR detection and 16S rDNA sequence analysis of different *Acidithiobacillus ferrooxidans* isolates. Biotechnol. Biotechnol. Equip. 25 (Suppl. 1), 47–49.

Jones, F.S., Bigham, J.M., Gramp, J.P., Tuovinen, O.H., 2014. Synthesis and properties of ternary (K, NH4, H3O)-jarosites precipitated from *Acidithiobacillus ferrooxidans* cultures in simulated bioleaching solutions. Mater. Sci. Eng. C 44, 391–399.

Kasozi, G.N., Nkedi-Kizza, P., Li, Y., Zimmerman, A.R., 2012. Sorption of atrazine and ametryn by carbonatic and non-carbonatic soils of varied origin. Environ. Pollut. 169, 12–19.

Kang, Y.W., Hwang, K.Y., 2000. Effects of reaction conditions on the oxidation efficiency in the Fenton process. Water Res. 34 (10), 2786–2790.

Khan, E., Wirojanagud, W., Sermsai, N., 2009. Effects of iron type in Fenton reaction on mineralization and biodegradability enhancement of hazardous organic compounds. J. Hazard. Mater. 161 (2–3), 1024–1034.

Kolpin, D.W., Thurman, E.M., Linhart, S.M., 1998. The environmental occurrence of herbicides: the importance of degradates in ground water. Arch. Environ. Contam. Toxicol. 35 (3), 385–390.

Lopez, A., Mascolo, G., Tiravanti, G., Passino, R., 1997. Degradation of herbicides (ametryn and isoproturon) during water disinfection by means of two oxidants (hypochlorite and chlorine dioxide). Water Sci. Technol. 35 (4), 129–136.

Meruane, G., Vargas, T., 2003. Bacterial oxidation of ferrous iron by *Acidithiobacillus ferrooxidans* in the pH range 2.5–7.0. Hydrometallurgy 71 (1–2), 149–158.

Pappu, A., Saxena, M., Asolekar, S.R., 2006. Jarosite characteristics and its utilisation potentials. Sci. Total Environ. 359 (1–3), 232–243.

Sangami, S., Manu, B., 2017. Synthesis of Green Iron Nanoparticles using Laterite and their application as a Fenton-like catalyst for the degradation of herbicide Ametryn in water. Environ. Technol. Innov. 8, 150–163.

Sangami, S., Manu, B., 2016. Fenton's Treatment of Actual Agriculture Runoff Water Containing Herbicides. Water Science and Technology, wst2016538.

Tan, G.L., Shu, W.S., Hallberg, K.B., Li, F., Lan, C.Y., Huang, L.N., 2007. Cultivation-dependent and cultivation-independent characterization of the microbial community in acid mine drainage associated with acidic Pb/Zn mine tailings at Lechang, Guangdong, China. FEMS Microbiol. Ecol. 59 (1), 118–126.

Wang, Y.S., Duh, J.R., Lin, K.Y., Chen, Y.L., 1996. Movement of three s-triazine herbicides atrazine, simazine, and ametryn in subtropical soils. Bull. Environ. Contam. Toxicol. 57 (5), 743–750.

Wang, H., Bigham, J.M., Tuovinen, O.H., 2006. Formation of schwertmannite and its transformation to jarosite in the presence of acidophilic iron-oxidizing microorganisms. Mater. Sci. Eng. C 26 (4), 588–592.

Wang, H., Liu, S., Liu, X., Li, X., Wen, Q., Lin, J., 2014. Identification and characterization of an ETHE1-like sulfur dioxygenase in extremely acidophilic Acidithiobacillus spp. Appl. Microbiol. Biotechnol. 98 (17), 7511–7522.

Woods, J., Mellon, M., 1941. Thiocyanate method for iron: a spectrophotometric study. Ind. Eng. Chem. Anal. Ed. 13 (8), 551–554.

Wood, A.P., Kelly, D.P., 1993. Reclassification of Thiobacillus thyasiris as Thiomicrospira thyasirae comb. nov., an organism exhibiting pleomorphism in response to environmental conditions. Arch. Microbiol. 159 (1), 45–47.

Wu, X., Liu, L., Zhang, Z., Deng, F., Liu, X., 2014. Phylogenetic and genetic characterization of Acidithiobacillus strains isolated from different environments. World J. Microbiol. Biotechnol. 30 (12), 3197–3209.

Yan, S., Zheng, G., Meng, X., Zhou, L., 2017. Assessment of catalytic activities of selected iron hydroxysulphates biosynthesized using *Acidithiobacillus ferrooxidans* for the degradation of phenol in heterogeneous Fenton-like reactions. Separ. Purif. Technol. 185, 83–93.

Yang, X., Wang, S., Liu, Y., Zhang, Y., 2014. Identification and characterization of *Acidithiobacillus ferrooxidans* YY2 and its application in the biodesulfurization of coal. Can. J. Microbiol. 61 (1), 65–71.